

OMAE2009-79502

CFD AS A DESIGN TOOL FOR HYDRODYNAMIC LOADING ON OFFSHORE STRUCTURES

Sampath Atluri, Allan Magee, Kostas Lambrakos

Technip USA
Houston, Texas, USA

ABSTRACT

Time-domain numerical integration of the rigid body equations of motion is a popular choice for analyzing the global motions of a single or multi-module floating platform. Potential flow theory cannot accurately account for all the hydrodynamic forces on certain components of the platform. However, for practical analysis, these members can be modeled as Morison members in the time-domain simulations. Computational Fluid Dynamics (CFD) can be used to calculate Morison coefficients for the given flow conditions on the exact geometry of the member.

This paper presents the results from CFD simulations performed on several individual components of a floating platform (like heave plates, truss members etc.,) in realistic environment conditions. The procedure used for extracting the linear and non-linear coefficients from the total calculated hydrodynamic force is also explained. Results from CFD are compared to existing published experimental results. Differences between full-scale and model-scale results will be emphasized where important. Some of the advantages of using CFD as opposed to model tests are highlighted.

INTRODUCTION

Motion of an offshore platform in waves can be reduced by increasing the hydrodynamic damping forces in the direction of motion. It is known that the hydrodynamic damping properties of a structure can be greatly improved by adding passive damping devices to the structure. One such example is the usage of damping/heave plates to the truss section of a typical Truss Spar platform as shown in Figure 1. These thin

rectangular / square plates (typical thickness to side ratio on a Spar is 1:80) are oriented horizontally and fitted at several vertical elevations of the truss. The heave plates control the heave motion of the platform by trapping water thereby increasing the total vertical added mass (inertia) of the system and also by inducing viscous effects from flow separation and vortex shedding, known as viscous drag. Of interest is the size of the plates, thickness and spacing between the plates for practical heave motion calculations and structural loads. A natural starting point to estimate the effect of the damping plates is to understand the hydrodynamic behavior of the isolated plates in oscillatory flow or plates oscillating in otherwise quiescent fluid. For oscillatory flows, two non-dimensional parameters are important, the Keulegan-Carpenter number $KC = U_m T / L$ and the Reynolds number $Re = U_m L / \nu$. Here U_m is the maximum relative velocity during oscillation, L is representative length (side of the plate), T is period of oscillation and ν is the kinematic viscosity of the fluid. Often, the KC number and the Reynolds number are combined to form a single non-dimensional parameter $\beta = Re / KC = L^2 / \nu T$. The inline hydrodynamic force (F) is usually represented by Morison's equation as

$$F = C_D * (0.5 * \rho * L^2) * U|U| + C_M * (\rho * L^3) * \dot{U} \quad (1)$$

where,

- C_D is the normalized drag coefficient
- C_M is the normalized inertial coefficient
- C_A is the normalized added mass coefficient

ρ is the density of the fluid
 U is the relative velocity between structure and fluid
 \dot{U} is the relative acceleration of the plate/fluid

In equation (1), the first term represents the viscous damping forces and the latter represents inertial force. For a harmonically oscillating flow, the KC number can be represented as $KC = 2 * \pi * A_0 / L$. Here A_0 is the amplitude of oscillation.

Most of the oscillatory flow studies in the literature concentrate on flow past cylinders. There is relatively little information on oscillatory flow past thin plates. The pioneering work in this field was done by Keulegan and Carpenter [1], who studied oscillatory flow past two dimensional flat plates and circular cylinders. Ref. [1] concluded that for flows in KC range from 2 to 100, C_D and C_M are functions only of KC and do not depend significantly on Re. More recently, several experiments [2][3] and flow visualization studies [4][5] addressed the thin edged oscillating plate problem in detail especially at low KC numbers. KC numbers in the range 0.01 to 1.0 represent the typical range of conditions for heave plates on a Spar platform.

Ref. [6] shows that truss spar heave motions remain small even for the most severe environments. For practical analysis, the heave motions are not sensitive to the choice of heave plate coefficients except in the 1000-year hurricane (survival condition). With the increased metocean criteria [7], both significant wave height and spectral peak periods have increased. What was formerly the survival event has become essentially the extreme (100-year environment). Also, the use of riser tensioners which shorten the heave natural period, increase the importance of understanding the hydrodynamic behavior of these plates for the given environmental conditions.

Finally, the heave plates may have several cutouts to accommodate risers and other equipment. These cutouts are generally considered to increase viscous damping but reduce inertia. These requirements may change over the course of a project and it is important to have quick and reliable tools available to assess the impact of potential design changes without the need for long-lead time, dedicated model tests.

The purpose of this paper is demonstrate that CFD can be used as an effective design tool to calculate the hydrodynamic forces on individual components of an offshore structure like heave plates, keel tank, etc., resulting in non-dimensional damping coefficients which could be used in other conventional time domain analysis tools. The following sections show results from several CFD calculations performed with single and multiple plates for a range of KC and Re numbers. Some results for more realistic configurations for

heave plates and other components are also shown towards the end.

NUMERICAL CALCULATIONS

Two types of oscillations were simulated in this work. Free decay oscillation and forced oscillation. In free decay oscillation, the structure is modeled as a spring suspension system. The CFD solver internally solves for the rigid body displacement and updates the boundary conditions for the Navier-Stokes equations at each time step. The mass of the plate and stiffness of the spring are adjusted such that the natural period of the system is reasonable (e.g. 2-3 seconds corresponding to model scale heave natural period). At the beginning of the simulation, the plate is displaced in the heave direction and released. The plate is restricted to move only in the heave direction (mesh velocity is made zero in other directions). The force acting on the moving plate is output from the solver as an integrated sum of pressure and shear stress. Since the complete N-S equations are solved, there is no need for special consideration of added mass or damping. The force obtained from the solver is purely hydrodynamic. In a forced harmonic oscillation, the displacement of the body is user specified (sine curve in this case) and hence no mass/stiffness information is required.

For all the simulations, the plate is completely submerged in water. The flow domain is about 7-10 times the length of the plate in any direction. No slip boundary condition is applied on the surface of the plate. The free body motion of the plate within the mesh is accommodated using a specified mesh boundary condition. The location of each node is specified based on the position of the plate at every time step. This approach avoids the solution of nodal locations using an arbitrary elastic solid to represent the mesh (Arbitrary Lagrangian Eulerian or ALE method) and hence solve for the new nodal locations. However, the fluid flow is calculated based on the new nodal locations as in the ALE method. Mesh points in the near vicinity of the plate are forced to retain their relative position with respect to the plate to ensure consistent quality of the mesh throughout the simulation. A representative mesh is shown in Figure 2. The mesh is unstructured and tetrahedral. Mesh elements on the surface of the body are triangles. Mesh points are arranged densely near the edges of the plate and across the thickness of the plate as shown in Figure 2. For all the oscillating plate results shown below, a minimum of six mesh points are maintained across the thickness of the plate. This resolution is found to be sufficient as shown in later sections (Figure 11). The mesh density around the plate is controlled by specifying the density transition. Near the surface of the plate, anisotropic tetrahedral elements are created for better resolution.

All CFD calculations were done using AcuSolve™. It is a fully implicit, finite element solver based on Galerkin Least

Squares formulation. Time step increment is constant throughout the simulation. A minimum of 400 time steps per each oscillation period (for forced and free oscillations) is imposed. Turbulence is modeled using Spalart's Delayed detached eddy simulation (DDES) [8]. No wall functions were used to calculate flow near the wall. It is observed from runs with and without turbulence that for low Reynolds and KC numbers modeling turbulence is not necessary. The total hydrodynamic force computed for the plate with or without turbulence shows no difference. As a special case to validate oscillating plate simulations, uniform flow past a fixed plate was simulated. Figure 3 shows the mean drag coefficient for a thin plate oriented at various angles of flow incidence. It may be noted that except in the 'stall' region, the drag coefficient matched very well with the experiments [9].

EXTRACTING MORISON – TYPE COEFFICIENTS

Extracting the Morison's coefficients from the total force calculated is difficult because the drag coefficient C_D is not well defined as $KC \rightarrow 0$. Contribution of the drag term in the total hydrodynamic force is minimal at very low KC numbers. Several methods of separating drag and inertia coefficients exist but none seems clearly superior. The simplest way to obtain the drag coefficient is to identify the force corresponding to the time instant of zero acceleration and equate it to the drag term of the Morison equation. Similarly, added mass coefficient can be obtained by identifying force corresponding to the instant of zero velocity. The authors of [10] and [11] used a linearized relationship between log-decrement of damping and quadratic viscous drag coefficient to compute the drag coefficient. Another method also used in [10] is to fit the force curve using the least squares error approach for the unknown coefficients, C_D and C_A . The motions and loads of the flow can be readily obtained from the CFD solver. Alternatively, the forces can be separated in the frequency domain [4][12]. For the current analysis, least squares error approach is used. A 10% difference between the total CFD force and the Morison force obtained from least squares error approach (maxima or standard deviation) is noticed at $KC \sim 1.0$. The difference varies linearly to zero as $KC \rightarrow 0$.

RESULTS

Free Decay of Multiple Plates

Following the experiments from [10] and [11] a series of calculations were performed to study the hydrodynamic coefficients for multiple heave plates as the spacing between the plates is varied. Three plates each one foot square and one quarter inch thick, mounted as shown in Figure 4 were considered. A set of three plates with holes in them was also

considered as shown. Spacing (H) between the plates is varied in three steps 0.5L, 1.0L and 2.0L. In all the tests, the tandem plates are given an initial heave displacement of about 0.5 ft.

In a free decay oscillation, the KC number and the Reynolds number changes continuously. Hence the coefficients were estimated separately for each oscillation period and listed against the corresponding KC number. The coefficients for solid plates are shown in Figures 5 and 7. The coefficients for holed plates are shown in Figures 6 and 8. For the least spacing case ($H/L = 0.5$), the drag coefficient for the center plate is significantly less than that of the end plates. As the spacing increases, drag on the center plate catches up with the other two. Variation in added mass follows the same trend but the variation is not as significant. Similar trends can be noted for plates with holes. The drag coefficients for plates with holes is very close compared to that of the solid plates especially for $KC = 0.5 - 2.5$. Also, the drag coefficients for all the plates increase with the spacing between the plates. An interesting trend to note is the small bump in drag coefficients for KC numbers between 1 and 1.5.

The added mass coefficients increase from 0.5 to 1.0 and the drag coefficients decrease from 7.0 to 1.0 as the KC number is varied between 0.5 and 2.5. Similar to the drag coefficient trends, the added mass coefficients for all the plates increase with the spacing between the plates. Added mass coefficients for holed plates are either close to or slightly lower to that of the solid plates. At plate spacing $H/L = 2.0$, both drag and inertia coefficients are same for all three plates.

Added mass coefficients for the center plate are compared to the average (of the three plates) added mass from the experiments [11] and shown in Figure 9. The calculated coefficients are in reasonable agreement with the experiments.

Forced and Free Oscillation of Single Plate

Forced Oscillation:

A single square plate is forced to oscillate sinusoidally at a prescribed frequency and amplitude and forces acting on the plate were calculated. In each simulation, the KC number remains constant throughout the simulation unlike in the free decay tests. Results are shown in Figures 10 and 11. Hydrodynamic coefficients are plotted as the KC number is varied. Other parameters varied are the Reynolds number or the β parameter, thickness of the plate and the shape of the plate (squared or circular).

The added mass coefficient of the plate increases slightly with the KC number (Figure 10). These results are generally consistent with design practice values. Drag coefficient decreases with increasing KC number (Figure 11). This is consistent with [4]. The C_D for all the plates tested and for all

the oscillating conditions converge to around 6 as KC number reaches 1.

To study the impact of Reynolds number on these coefficients, two plate sizes were considered: (a) a 2ft x 2ft plate ($L/t \sim 200$; $\beta = 1.9e^5$) which will be called model scale plate and (b) a 98ft x 98ft plate ($L/t \sim 150$; $\beta = 4.5e^8$) which will be called full scale plate. Both the plates are forced to oscillate in the same KC range. The C_D and C_A values are unaffected by the change in Reynolds number. Convergence of the computation is verified by results from using a coarse mesh for the full scale plate. The coarse mesh had 3 mesh points across the thickness of the plate whereas the finer mesh which was used in all the calculations shown here had 6,7 or 8 points. The volume mesh is refined accordingly.

The thickness of a plate seems to consistently influence the drag coefficients as can be seen in Figure 11. The thinner the plate, the higher the drag observed. The difference is more significant for $KC < 0.5$ and this is indicated by both CFD calculations and experimental data [4]. And finally, CFD simulation of forced oscillation of circular plates ($L/t \sim 87.5$ and $L/t \sim 37$) gave C_D of 10.0 and 6.4; C_A of 0.58 and 0.57. These results match very closely with [4].

Free Oscillation:

Figures 10 and 11 also show results for a single plate ($L/t \sim 48$) in heave decay. The problem setup is similar to the free decay tests from previous section. C_D and C_A are plotted against a representative KC number for each oscillation. The coefficients vary similarly as in the forced oscillations with KC number. One forced oscillation calculation with the same plate ($L/t \sim 48$) gives the same drag coefficient as free oscillation.

As a general conclusion, the drag coefficient in general is a function of both the thickness of the plate as well as the KC number.

Realistic Heave Plate / Bluff Body Oscillation

CFD has been used to calculate the hydrodynamic coefficients for more realistic Truss Spar components. Figure 12 shows the schematic of a heave plate and a keel tank as built on a model scale Truss Spar Platform. Holes on the face of a heave plate are common to accommodate risers and other equipment. Four corner legs of the truss are also modeled for heave plate simulations to account for appropriate flow behavior near the corners of the plate. Figure 13 shows the schematic of a cylinder with strakes. This represents the hard tank of a model scale Truss Spar. To obtain the hydrodynamic coefficients in the heave direction, each component is forced to oscillate sinusoidally in the heave direction at prescribed amplitude and frequency representing a particular KC number.

The simulation procedure is similar to that of the plain plate cases discussed above. The total hydrodynamic force obtained from the numerical calculations is used to generate Morison coefficients as done with the plain plates. Selected results for the Spar components are shown in Table 1. The results show C_D and C_A for components oscillating at one KC number only but it also demonstrates that CFD can be readily used for realistic Spar components.

CONCLUSIONS AND DISCUSSION

CFD was used to estimate the hydrodynamic coefficients of oscillating bodies in a fluid. Damping coefficients for realistic heave plates, keel tank, etc., were estimated. An attempt was made to correlate the coefficients for square plates and circular with previous experiments. For very thin plates, ($L/t > 150$), the added mass coefficient nor the drag coefficient change significantly with the Reynolds number. C_D could change significantly with KC number as seen in the results. Drag and added mass coefficients estimated from forced-oscillation simulations compare well with coefficients from other known forced oscillation experiments. It can be concluded that analyzing plate hydrodynamics should also involve the thickness of a plate as a dependant parameter. This study has demonstrated that CFD can be used effectively to calculate the hydrodynamic force on specific components of structures.

CFD analyses can be performed quickly. For example, a forced oscillation run for a model scale heave plate (with half a million mesh points) required less than 6 hours on a 32 processor cluster. The turnaround time for a set of analysis runs is much less than building and testing a physical model, and this allows reliable assessment of design variations to be performed numerically, so that confirmatory model tests, if still required, can be limited to a single target configuration. Furthermore, the ability to readily repeat the CFD analysis at full scale Reynolds numbers extends its capabilities beyond those of reduced scale physical tests.

NOMENCLATURE

CFD – Computational Fluid Dynamics
GOM – Gulf of Mexico

ACKNOWLEDGEMENT

The authors wish to thank Technip for permission to publish this work.

REFERENCES

[1] Keulegan, G.H. and Carpenter, L.H. "Forces on Cylinder and Plates in an Oscillating Fluid", Journal of Research of the National Bureau of Standards, Vol 60, pp. 423-440, 1958.

[2] Troesch, A., et al "Hydrodynamics of thin plates: First year JIP report", University of Michigan 1999.

[3] Troesch, A., et al "Hydrodynamics of thin plates: Second year JIP report", University of Michigan 2000.

[4] He, H., Troesch, A., Perlin, M. "Hydrodynamics of damping plates at small KC numbers", IUTAM Symposium on Fluid-Structure Interaction in Ocean 2007.

[5] Tao, L. and Thiagarajan, K., "Low KC flow regimes of oscillating sharp edges, Applied Ocean Research, Vol 25, p21 - 35, p53 - 62.

[6] Magee, A., A. Sablok, J. Maher, J.Halkyard, L. Finn, I. Datta, "Heave Plate Effectiveness in the Performance of Truss Spars", OMAE2000-4230.

[7] API RP 2INT-MET, "Interim Guidance on Hurricane Conditions in the Gulf of Mexico," May 2007.

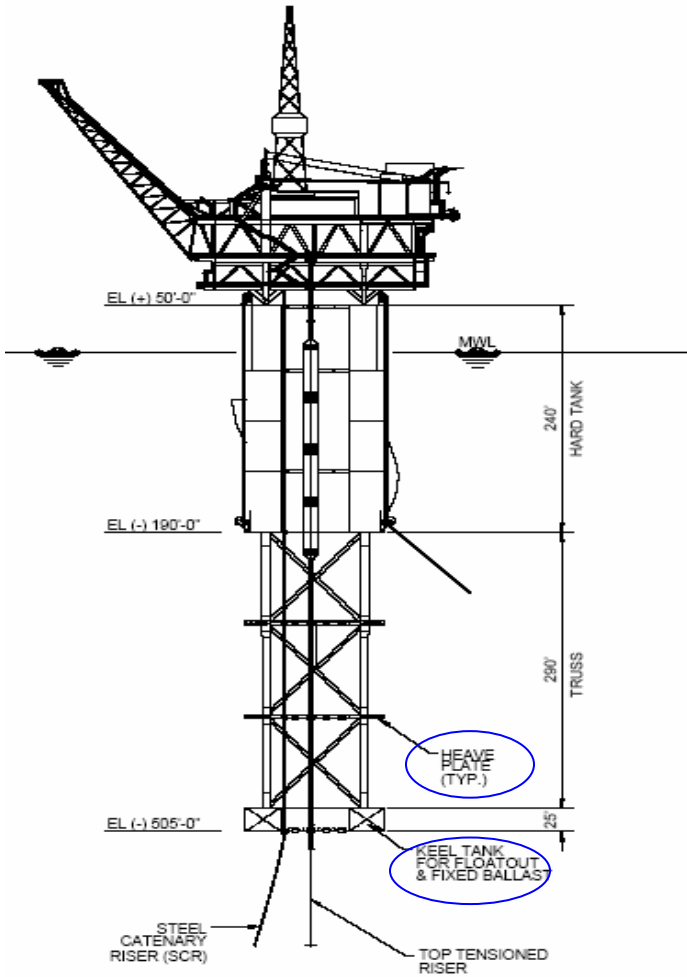
[8] Spalart, P., et al "A new version of Detached-Eddy Simulation, resistant to ambiguous grid densities", Theoretical and Computational Fluid Dynamics. 20: 181-195, 2006.

[9] Blevins, R., "Applied Fluid Dynamics Handbook", 2003.

[10] Prislin, I., Blevins, R., Halkyard, J. "Viscous damping and added mass of solid square plates", 17th International Conference on OMAE 1998.

[11] Prislin, I., Halkyard, J. "Model test Report: Viscous damping and added mass of a square plate", Deep Oil Technology Inc., 1997.

[12] Bendat and Piersol, "Decomposition of wave forces into linear and non-linear components", Journal of Sound and Vibration, Vol 106, 1986.



TRUSS SPAR

Figure 1: Layout of a typical Truss Spar showing Heave plates and Keel tank.

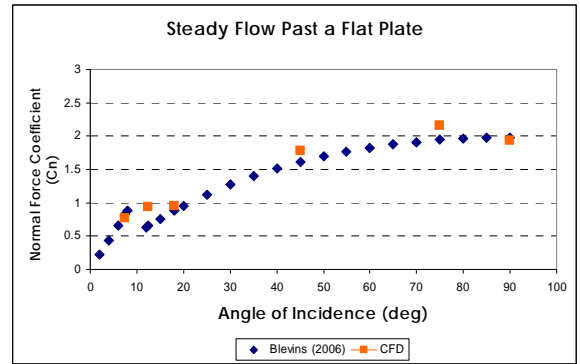


Figure 3: Uniform flow past a flat plate at various incidence angles.

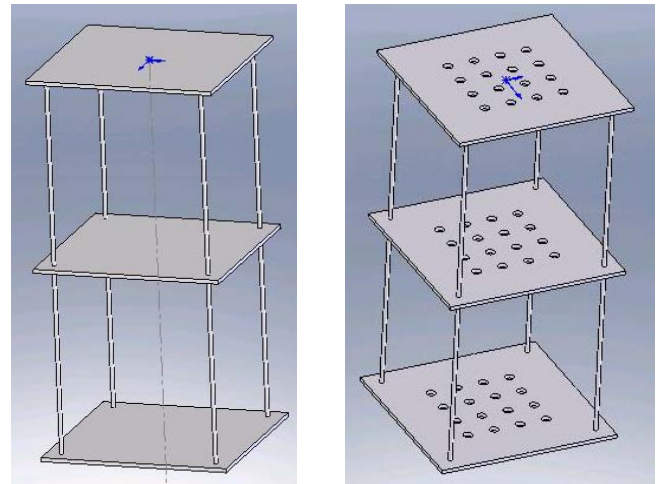


Figure 4: Three heave plate test configuration

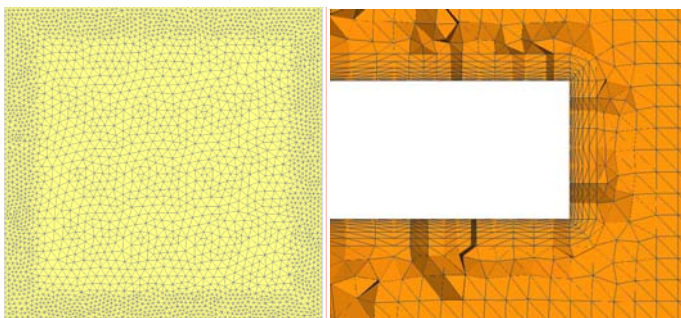


Figure 2: Surface mesh (left) and near wall volume mesh (right) for the plate.

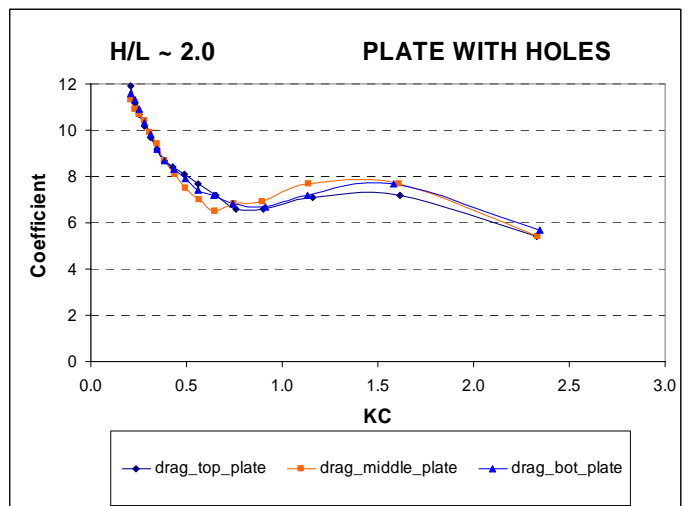
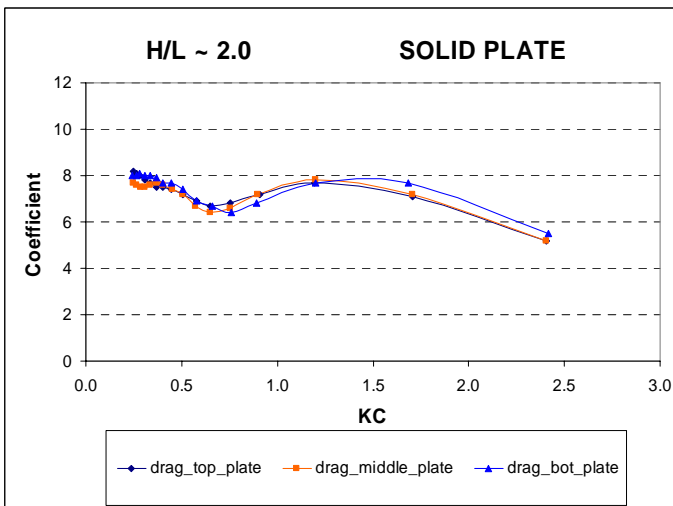
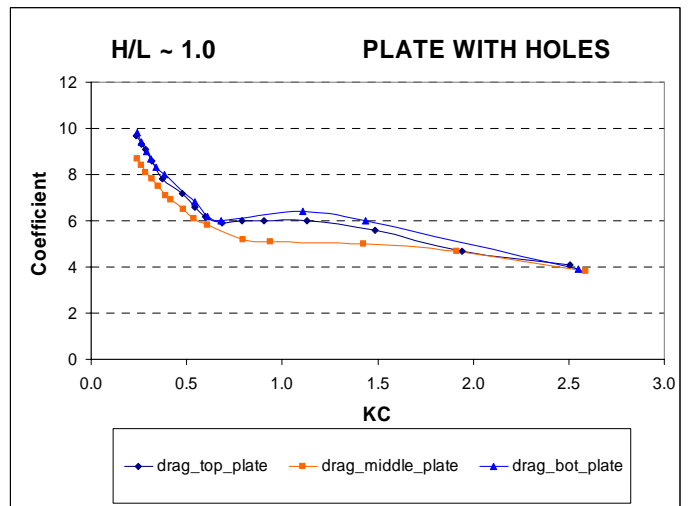
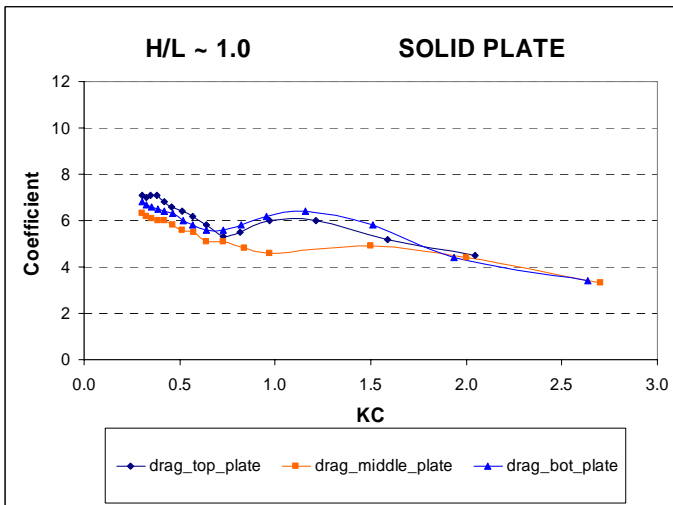
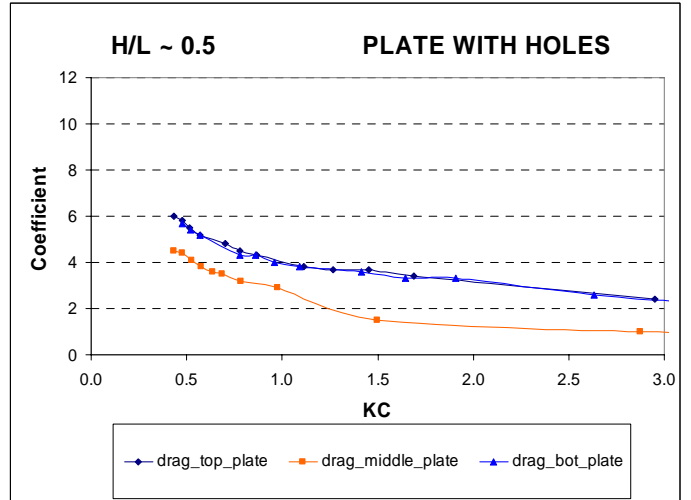
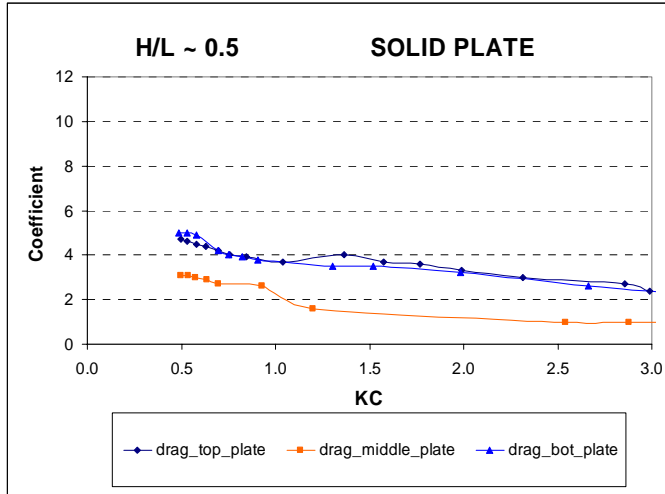


Figure 5: Drag coefficients for the three plate (solid) configuration.

Figure 6: Drag coefficients for the three plate (holed) configuration.

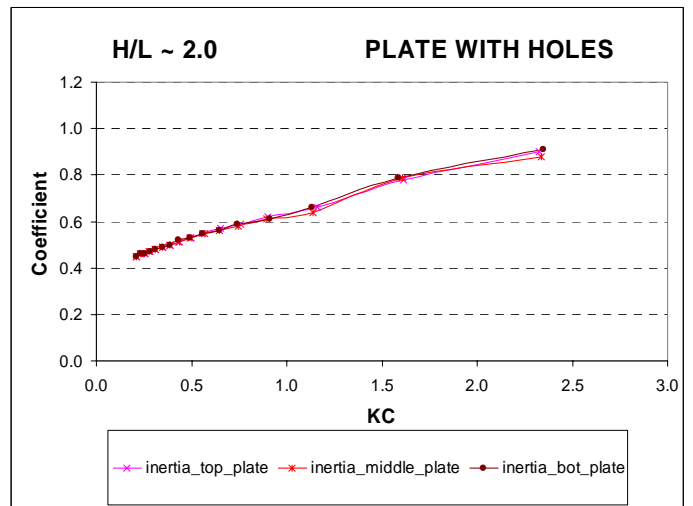
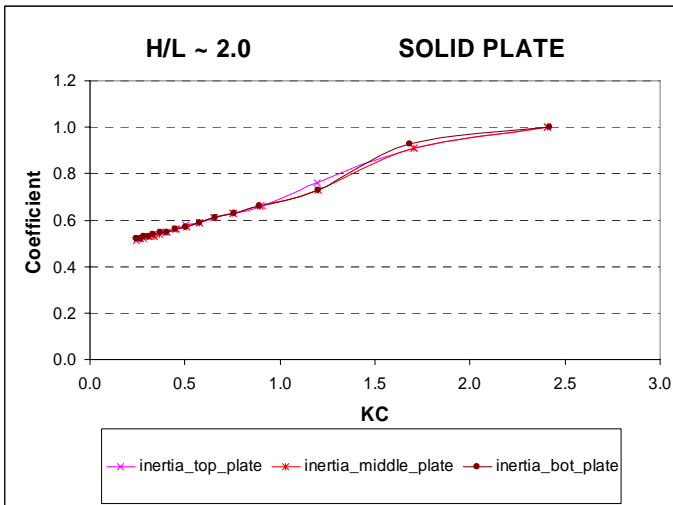
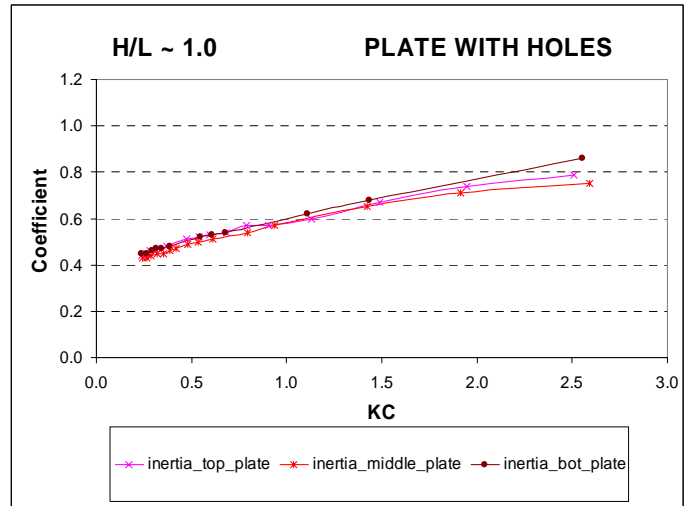
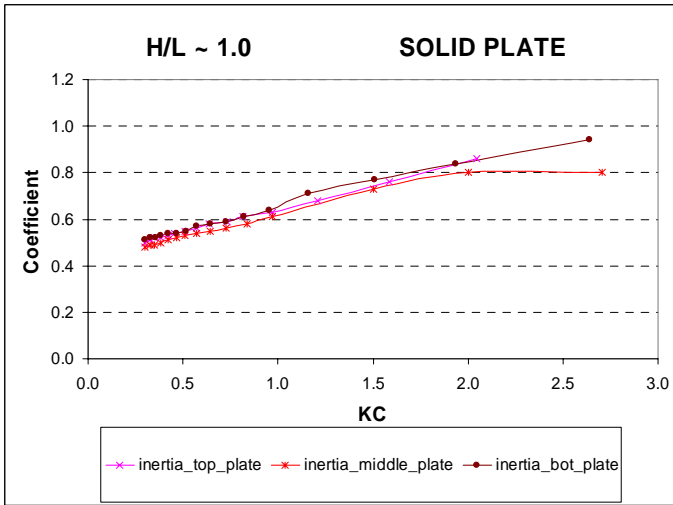
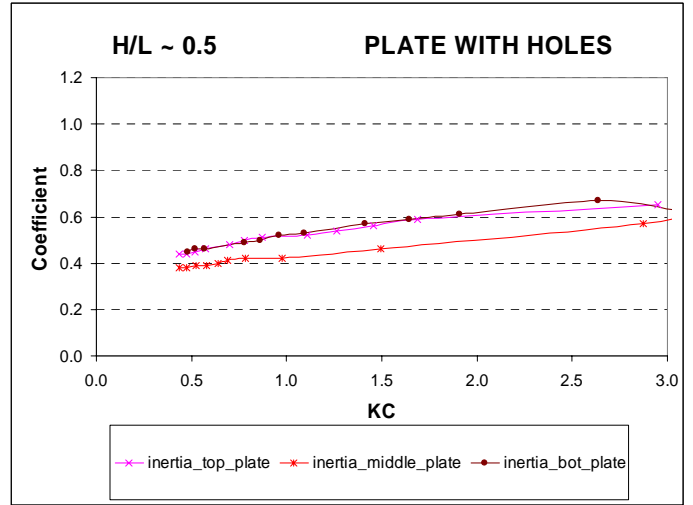
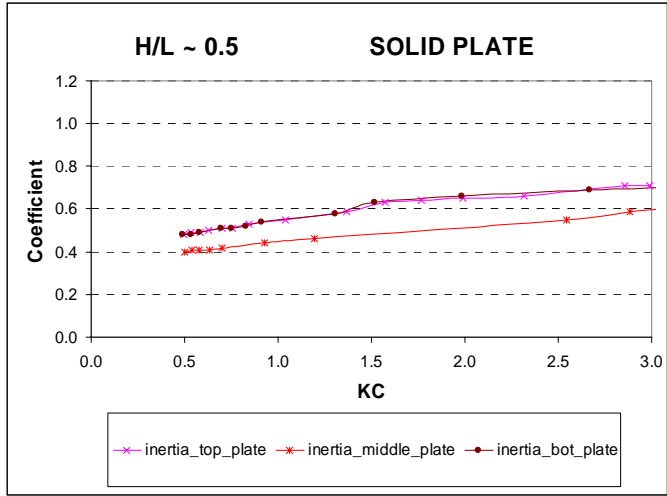


Figure 7: Inertia coefficients for the three plate (solid) configuration.

Figure 8: Inertia coefficients for the three plate (holed) configuration.

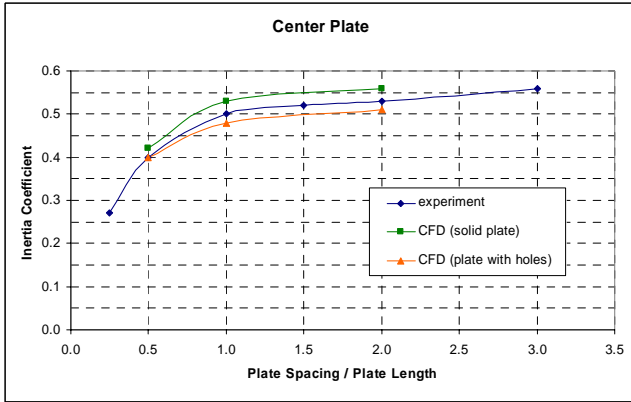


Figure 9: Inertia coefficient variation with plate spacing.

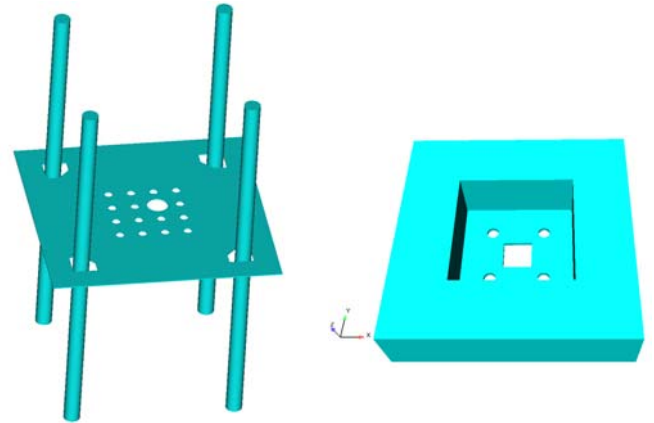


Figure 12: Heave Plate and Soft tank geometries close to as-built configurations

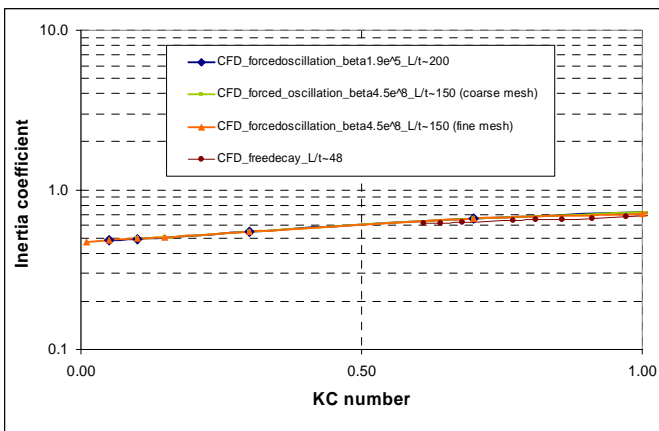


Figure 10: Inertia coefficients for single square plate in forced oscillation

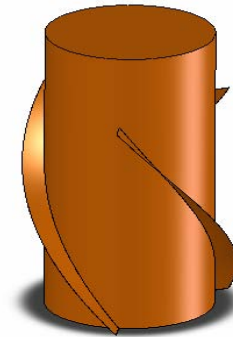


Figure 13: Straked cylinder resembling the hard tank of a Spar

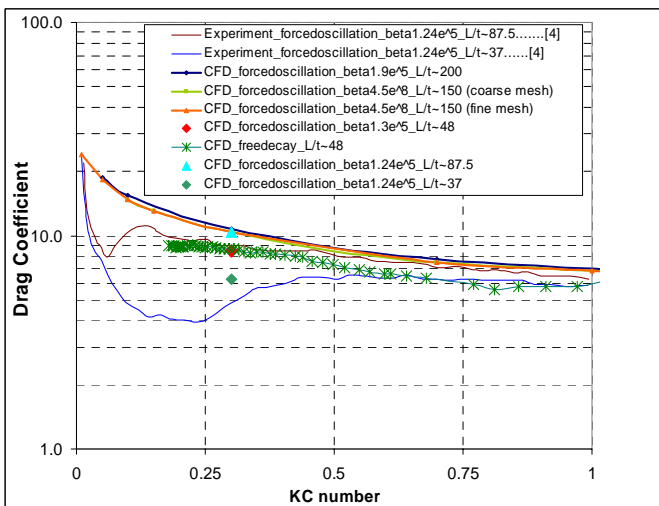


Figure 11: Drag coefficients for single square plate in forced oscillation.

Table 1: Hydrodynamic coefficients for realistic geometries

<i>(model scale)</i>	KC	C _D	C _A
Heave Plate	0.36	12.1	0.52
Keel tank	0.3	7.5	3.49
Straked cylinder*	0.05	7.5	0.47

*Representative length for KC is the diameter of the cylinder